

Crystal-field excitations in CeCu_2Si_2

E. A. Goremychkin

Laboratory of Neutron Physics, Joint Institute for Nuclear Research, Dubna, Head Post Office, P. O. Box 79, Moscow, Russia

R. Osborn*

ISIS Science Division, Rutherford Appleton Laboratory, Chilton, Didcot, Oxon, OX11 0QX, United Kingdom

(Received 6 January 1992; revised manuscript received 22 October 1992)

An inelastic-neutron-scattering investigation of the dynamic magnetic susceptibility of the heavy-fermion compound CeCu_2Si_2 is presented. We find evidence for only one crystal-field (CF) transition at 30 meV in addition to quasi-elastic-scattering implying a doublet-quartet level scheme in agreement with specific-heat results but in contradiction with two earlier neutron-scattering studies. Using other experimental results, we propose a set of CF parameters ($B_2^0 = -1.29 \pm 0.06$ meV, $B_4^0 = (-4.3 \pm 0.2) \times 10^{-3}$ meV, $|B_4^4| = 0.45 \pm 0.02$ meV) which describe satisfactorily all the measured properties that depend on the CF. A simple CF model is adequate to describe most of the observed features of this system at temperatures well above the Kondo temperature although the width of the observed transition is anomalously large. A comparison of the CF parameters with other isostructural compounds gives the clearest evidence so far that hybridization between the cerium f electrons and the silicon p electrons is mainly responsible for the CF potential itself.

I. INTRODUCTION

The discovery of superconductivity below $T_c = 0.5$ K in the heavy-fermion compound CeCu_2Si_2 (Ref. 1) has stimulated many experimental investigations of its bulk and microscopic properties in the ensuing decade.^{2,3} Of particular significance was the observation that the specific-heat discontinuity at T_c is enhanced by a factor of 10^3 over conventional superconductors, the same amount as the normal-state electronic specific-heat coefficient ($\gamma = 1.1$ J/mol/K²), thereby confirming that the heavy fermions are responsible for the superconductivity. It is now generally accepted that the large mass enhancements arise from the hybridization of the cerium f electrons with the conduction-band electrons, so that the f shell becomes partially delocalized and the Fermi liquid acquires some f character. However, the hybridization energies are relatively small, characterized by a Kondo temperature $T_K \sim 10$ K. At higher temperatures, CeCu_2Si_2 behaves like a localized f -electron system with an anisotropic Curie-Weiss susceptibility.^{4,5}

In common with nearly all rare-earth systems, the crystal-field (CF) potential of heavy-fermion compounds is an essential component in determining their measured thermodynamic and magnetic properties (specific heat, magnetic susceptibility, transport properties, etc.). It determines the degeneracy and wave function of the f -electron ground state involved in the hybridization, and so is required in theoretical analyses that go beyond simple phenomenology.⁶ In addition, it has been proposed that the CF potential is itself largely due to the hybridization interaction between the localized f -electron states and band states that is responsible for the heavy-fermion behavior.⁷

The most direct method of determining the CF in a

metallic compound is inelastic-neutron scattering (INS), for which the cross section is proportional to the dynamic magnetic susceptibility. There have now been four INS studies of CeCu_2Si_2 ,⁸⁻¹¹ two of which proposed similar CF level schemes. In tetragonal symmetry, the $J = 5/2$ ground-state multiplet splits into three doublets. The first INS investigation⁸ (referred to hereafter as HO) concluded that the first excited doublet is at an energy of 12 meV with the second at 30 meV. A recent INS investigation, on nonstoichiometric $\text{CeCu}_{2\pm x}\text{Si}_2$ (Ref. 9) (referred to as HM), came to similar conclusions as HO concerning the CF level scheme although the position of the lower doublet was between 17 and 20 meV and appeared to depend strongly on the stoichiometry. The two other INS measurements using polarized neutrons observed a broad peak at about 30 meV but had insufficient resolution to confirm the presence of a peak at 12 meV.^{10,11}

The CF level scheme proposed by HO is controversial since the specific-heat data on CeCu_2Si_2 (Ref. 12) are only consistent with a doublet-quartet scheme, i.e., a ground-state doublet and two closely spaced excited doublets at an energy of about 30 meV, and a number of other investigations have questioned this result. The strong anisotropy of the single-crystal magnetic susceptibility^{4,5} requires a much larger value of the second degree CF parameter B_2^0 than deduced by HO. Analyzing these data, Kawakami *et al.*¹³ derive a ground-state wave function which differs markedly from that determined from the HO CF parameters, as do Maekawa *et al.*¹⁴ who show in addition that the measured resistivity is consistent with a doublet-quartet CF splitting. Finally, only one broad crystal-field peak has been observed in Raman spectroscopy at about 36 meV (Ref. 15).

The main challenge in interpreting measured neutron spectra is to derive correctly the phonon contribution ei-

ther by a careful analysis of the angular dependence of the scattering or by using an isostructural nonmagnetic compound (e.g., containing La instead of Ce). This is a particularly serious problem in the case of CeCu₂Si₂ since the nuclear, i.e., phonon cross section is very strong, especially below 20 meV (Ref. 16) in the energy range of the proposed central doublet. In the light of the above-mentioned discrepancies between INS and other studies, it is very important to assess the reliability of the earlier conclusions based on INS data.

We have therefore performed new measurements on stoichiometric samples of CeCu₂Si₂ and LaCu₂Si₂ on the neutron time-of-flight spectrometers HET, at the pulsed spallation neutron source ISIS (Rutherford Appleton Laboratory, U.K.), and KDSOG at the pulsed reactor IBR-2 (JINR, Russia). HET is a chopper spectrometer which combines very high energy-resolution with a wide range of energy transfer ϵ and wave-vector transfer Q . These characteristics allow us to estimate the magnetic contribution by a scaling procedure, described by Murani,¹⁷ which uses the low- and high- Q data of the La compound to determine the Q dependence of the CeCu₂Si₂ phonon contribution. The validity of this method has been confirmed by Monte Carlo simulations of the level of multiple phonon scattering, which dominates the inelastic nuclear contribution at low scattering angles. Measurements of CeCu₂Si₂ and LaCu₂Si₂ samples on KDSOG, an inverse geometry spectrometer with high intensity and moderate resolution, have allowed the use of direct subtractions because multiple scattering is much less significant in this scattering geometry. The complementary use of these two spectrometers with different methods of estimation of the magnetic scattering provides the justification for our main conclusions.

Our main result is that, contrary to the conclusions of previous INS investigations but in accord with the specific-heat results, there is only one CF transition at 30 meV, which is very broad. It has a Lorentzian line shape with a half-width of $\Gamma=8.4$ meV at 2 K. There is also evidence for magnetic quasielastic scattering (QES) with $\Gamma=1.9$ meV at 10 K, in good agreement with previous low-energy investigations.⁸ The combined tails of the

QES scattering and the broad inelastic scattering produce significant magnetic intensity in the range of 10 to 20 meV but this is not enough, in our view, to support the proposal of a second CF transition in this region.

The CF potential that we derive on the basis of these results is shown to arise mainly from the nearest-neighbor shell of silicon ions rather than the approximately equidistant shell of copper ions. This is a general feature of isostructural cerium compounds, whereas the copper shell appears to make the dominant contribution in the normal rare-earth compounds. This observation is, we suggest, the clearest evidence so far that anomalous hybridization of the $4f$ electrons with, in this case the silicon p electrons, is mainly responsible for the CF potential, as proposed by Levy and Zhang.⁷ By implication, f - p hybridization is also responsible for the heavy-fermion behavior of this compound.

In the next section, we present the cross section for magnetic neutron scattering from CF transitions. Section III gives details of the experimental procedure and Sec. IV describes the methods used to extract the estimated magnetic contribution. In Sec. V, we propose a CF model that is consistent with all known experimental data that depend directly on the CF potential and analyze the contributions of the different neighbor shells. We discuss our conclusions in Sec. VI.

II. MAGNETIC-NEUTRON-SCATTERING CROSS SECTION

In tetragonal symmetry, the CF Hamiltonian for Ce³⁺ ions is

$$\mathcal{H} = B_2^0 O_2^0 + B_4^0 O_4^0 + B_4^4 O_4^4, \quad (1)$$

where O_n^m are the Steven's operator equivalents and B_n^m are phenomenological CF parameters. This splits the $J=5/2$ ground-state multiplet into three Kramers doublets, Γ_{16} , $\Gamma_{17}^{(1)}$, and $\Gamma_{17}^{(2)}$. The neutron-scattering law for unpolarized neutrons in the dipole approximation is given by¹⁸

$$S(Q, \epsilon) = f^2(Q) \left[\frac{\epsilon}{1 - \exp(-\epsilon/kT)} \right] \left\{ \sum_m \chi_C^m F(\epsilon, \Gamma_{mm}) + \frac{1}{2} \sum_{m \neq n} \chi_{VV}^{mn} \left[1 - \exp\left(-\frac{\epsilon_{mn}}{kT}\right) \right] F(\epsilon - \epsilon_{mn}, \Gamma_{mn}) \right\}, \quad (2)$$

where $f^2(Q)$ is the Ce³⁺ form factor, χ_C^m and χ_{VV}^{mn} are the Curie and Van Vleck magnetic susceptibilities where m and n label the CF states [see Eqs. (16) and (17) of Ref. 18 for definitions of χ_C and χ_{VV} in the CF case], and $F(\epsilon, \Gamma)$ is a normalized function characterizing the line shape of the transition. In the present work, we assume a Lorentzian form for F , in which Γ is the half-width. Although different line shapes have been proposed for CF

transitions in heavy-fermion compounds,¹⁹ the Lorentzian form has been shown theoretically to be a reasonable approximation,^{20,21} particularly at high temperatures.¹⁹

III. EXPERIMENT

The samples of CeCu₂Si₂ and LaCu₂Si₂ were prepared by arc-melting of stoichiometric quantities of the constit-

uent elements, with no measurable weight loss, and annealing for one day at 700 °C. Both neutron and x-ray diffraction confirmed that the samples were single phase. The experiments on HET used 50 g of each compound sealed in thin-walled aluminum containers which were mounted on a closed-cycle refrigerator (CCR) for measurements down to 20 K and in a pumped helium flow cryostat for measurements at 2 K. The data were normalized on an absolute scale using a vanadium standard. Larger samples of 200 g, also sealed in aluminum containers, were used in the experiments on KDSOG which used a helium cryostat at temperatures of 10, 77, and 300 K.

HET is a direct geometry chopper spectrometer, in which the incident neutron beam is monochromated by a fast Fermi chopper which is phased to the source pulses. The scattered energy is determined by the neutron time-of-flight. The measurements were made with an incident energy of 60 meV using a chopper rotation speed of 500 Hz, giving an energy resolution of 1.5 meV full width at half-maximum (FWHM) at the elastic position, improving to 0.8 meV at $\epsilon=30$ meV. Figure 1 shows data measured at an average scattering angle $\phi=136^\circ$ on both CeCu_2Si_2 and LaCu_2Si_2 at a temperature of 20 K. This corresponds to a wave-vector transfer Q of 9.98 \AA^{-1} at $\epsilon=0$ so that the Ce^{3+} form factor $f^2(Q)=0.076$ and there is negligible magnetic intensity. Inspection of the data shows that there are large peaks in the phonon density of states (PDOS) at 13 and 18.5 meV in the Ce com-

pounds with smaller peaks at 33 and 38 meV. The La data are very similar, but the lower peaks are more intense and there are small energy shifts of all the features. The relative integrated intensities of the Ce and La data from 8 to 20 meV are consistent with the different scattering lengths of the two compounds if we assign these peaks mainly to combined rare earth and copper modes. However, the higher energy peaks have similar intensities in the two compounds consistent with assigning them mainly to silicon vibrational modes. The results are in good agreement with the generalized PDOS reported by Gompf *et al.*¹⁶ but the new spectra are better resolved.

Figure 2 shows the spectra measured at an average ϕ of 5° at 20 K. Qualitatively, the La spectrum is similar to the high-angle data with a small increase of spectral weight at higher-energy transfers. In contrast to this, the Ce spectrum has substantial extra scattered intensity over the whole measured energy range. The most obvious additional feature is a broad peak centered at about 30 meV. Since these spectra are at much lower Q [1.63 \AA^{-1} at $\epsilon=30$ meV, $f^2(Q)=0.870$], the extra scattering is clearly of magnetic origin. The histograms in Figs. 1 and 2 represent our estimate of the phonon contribution based on the Monte Carlo simulations to be described in the next section with the remaining scattering assigned to magnetic inelastic scattering. The strong nuclear elastic scattering prevents us from analyzing data

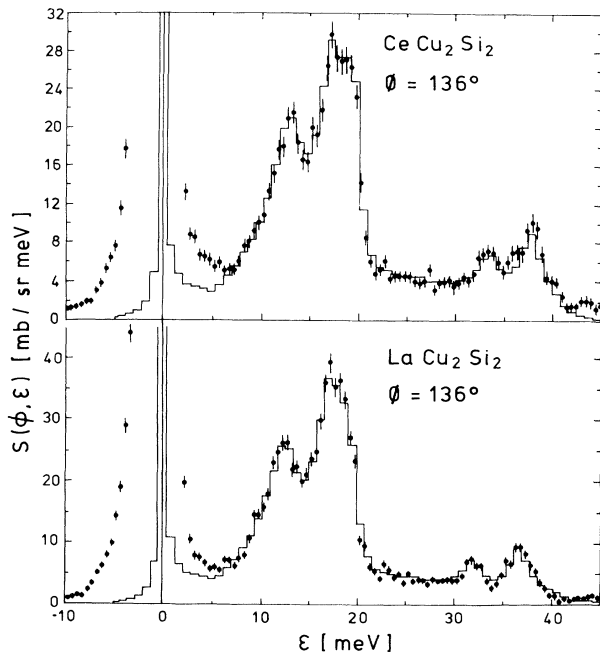


FIG. 1. Neutron energy spectra from (a) CeCu_2Si_2 and (b) LaCu_2Si_2 measured on HET with an incident energy of 60 meV and scattering angle of 136° (filled circles). The histograms are the total scattering determined by the Monte Carlo simulation. Note that the simulation has not been convolved with the instrumental resolution function so the elastic scattering is confined to one histogram bin.

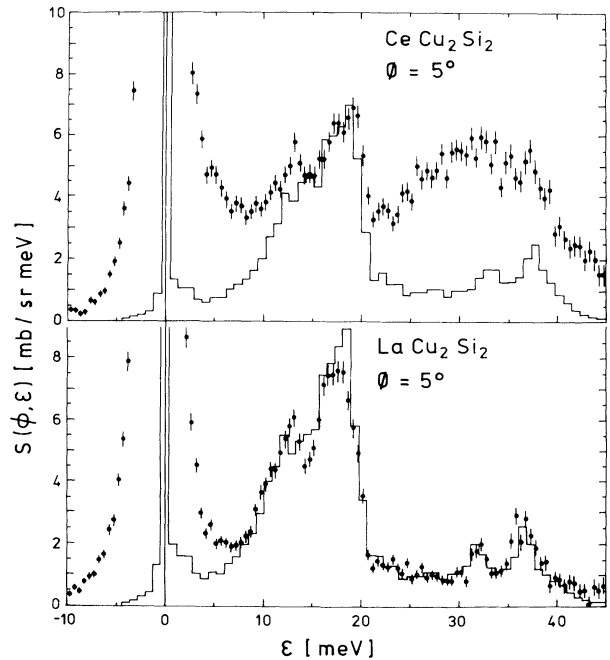


FIG. 2. Neutron energy spectra from (a) CeCu_2Si_2 and (b) LaCu_2Si_2 measured on HET with an incident energy of 60 meV and scattering angle of 5° (filled circles). The histograms are the total phonon scattering determined by the Monte Carlo simulation. Note that the simulation has not been convolved with the instrumental resolution function so the elastic scattering is confined to one histogram bin.

below 5 meV reliably, although there is evidence for a magnetic QES contribution whose tail extends to about 10 meV. The data taken in the helium cryostat at 2 K are qualitatively the same with a slight narrowing of the

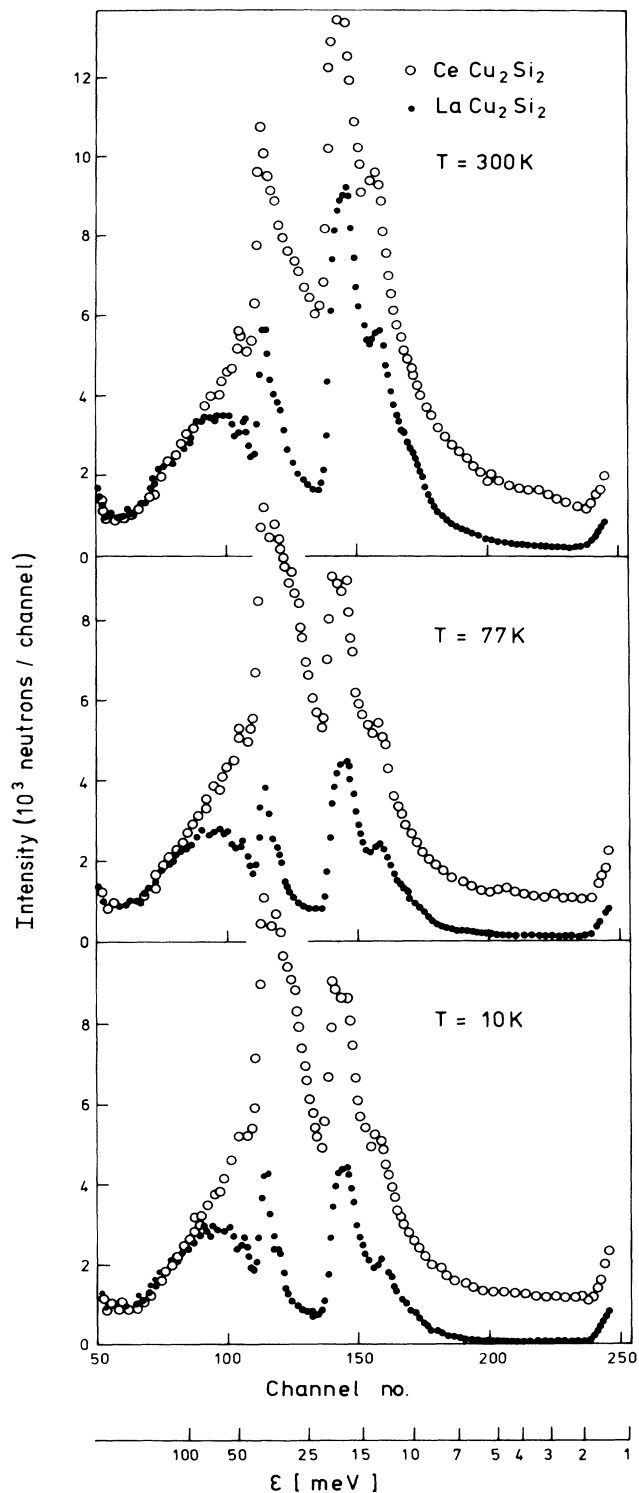


FIG. 3. Neutron time-of-flight spectra from CeCu_2Si_2 (open circles) and LaCu_2Si_2 (closed circles) at 10, 77, and 300 K, measured on KDSOG.

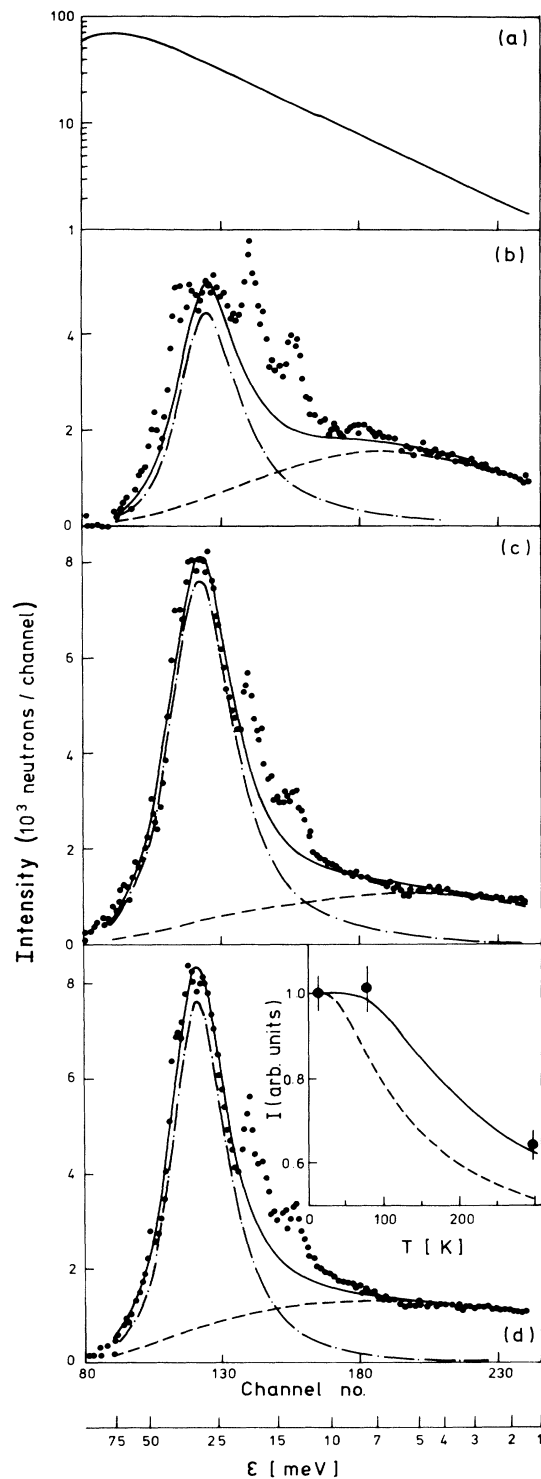


FIG. 4. (a) Energy dependence of the incident flux on KDSOG. The magnetic contribution to the neutron time-of-flight spectra on KDSOG determined by subtracting LaCu_2Si_2 data from CeCu_2Si_2 data at (b) 300 K, (c) 77 K, and (d) 10 K. The solid line is the total magnetic response composed of a quasi-elastic (dashed line) and inelastic (chain line) Lorentzian. The inset gives the temperature dependence of the inelastic line (points) compared to two CF models; the present model (solid line), HO (dashed line).

30 meV peak.

KDSOG is an inverse geometry time-of-flight spectrometer. This means that the sample is irradiated by a white beam produced by the pulsed reactor and the energy of the scattered beam is fixed at 4.9 meV by graphite analyzers placed behind cooled beryllium filters. Therefore, in contrast to HET, it is the incident energy which is determined by the total neutron time-of-flight. At the elastic line, the resolution is 0.6 meV but this worsens at high-energy transfer because of the large pulse widths from the moderator. KDSOG has good intensity in the energy range up to 100 meV but has the disadvantage that Q cannot be varied over a wide range, being defined mainly by the incident wave vector. The high- Q to low- Q scaling procedure used to analyze the HET data cannot therefore be used in this case so a direct subtraction (Ce–La) has been employed, the details of which are described in the next section.

Figure 3 shows the raw data for both the La and Ce compounds measured on KDSOG at 10, 77, and 300 K. We present the data as counts per time-of-flight channel without correcting for the energy dependence of the incident flux because it preserves the measured distribution of intensity and gives a clearer idea of the relative weights with which the different contributions are determined (magnetic QES, magnetic inelastic, and phonon). When transformed to $S(\phi, \epsilon)$ the data are consistent with the HET data of Fig. 2. It should be noted that because of the energy dependence of the spectrometer resolution, the QES is better defined than on HET but high-energy features, such as the two silicon mode peaks, are not so well resolved. Figure 4 shows the difference spectra (Ce–La) after correction for the different scattering lengths (see next section).

IV. DATA ANALYSIS

A. Correction for phonon scattering

The HET data are measured at both very low ϕ (5°) and very high ϕ (136°). There are also data at intermediate scattering angles ($\phi = 9^\circ$ to 29°) but the secondary flight path is shorter reducing the resolution, so we have not analyzed these spectra in detail. The high-angle data define the general shape of the phonon scattering and, in the incoherent approximation, is proportional to $Z(\epsilon)[1+n(\epsilon)]/\epsilon$, where $Z(\epsilon)$ is the generalized PDOS and $n(\epsilon)$ is the Bose factor. The intensity of this scattering should vary as $Q^2 e^{-2W}$, where e^{-2W} is the Debye-Waller factor, but the scattering at low angle is much stronger than estimates based on this Q dependence. In fact, the scattering at very low Q is nearly independent of Q for $\phi < 20^\circ$. The reason for this anomalous intensity at low angles is multiple scattering (MS), which is predominantly elastic plus single phonon, but also contains contributions from two-phonon and higher-order scattering processes. The former preserves the shape of the measured scattering, whereas the latter has the tendency to shift the spectral weight to higher energy transfers, particularly at low temperatures.

In order to estimate the amount of MS at low angles,

we have performed simulations using the Monte Carlo program DISCUS,²² which requires as input $S(Q, \epsilon)$ over a wide range of Q and ϵ . The 136° data, which are dominated by real single-phonon scattering when the incident energy is 60 meV, was used to provide an initial estimate of $Z(\epsilon)$. Ideally, $Z(\epsilon)$ should be separated into partial densities of state $Z_i(\epsilon)$ where i labels each type of atom in the unit cell, i.e., Ce or La, Cu, and Si. These are then weighted in total cross section by σ_i/M_i , where σ_i is the nuclear scattering cross section and M_i is the atomic mass. Therefore, as a refinement of the model, we have assumed that the peaks in the energy range 30 to 40 meV were due solely to silicon vibrational modes, but that below 25 meV, all the constituents have the same $Z_i(\epsilon)$. The integrals of the three $Z_i(\epsilon)$ are then normalized to one, and separately used to calculate $S_i(Q, \epsilon)$ in the incoherent approximation.²³ These are then combined to form a total $S(Q, \epsilon)$. The numerical method that we employed generates all orders of multiphonon scattering in addition to the single-phonon scattering.²⁴ In principle, the output from the Monte Carlo simulation may be used to improve the initial estimate of $Z_i(\epsilon)$, but the agreement with the 136° data was sufficiently good to make further iterations unnecessary (Fig. 1). This procedure was carried out for both CeCu_2Si_2 and LaCu_2Si_2 .

The simulations show that the MS for a moderately absorbing thin sample of slab geometry perpendicular to the incident beam is nearly isotropic except near $\phi = 90^\circ$. The reason for this is not hard to see. The first scattering process is likely to be into the plane of the sample, i.e., at 90° ;²⁵ it cannot then matter whether the second scattering process is in the forward or backward direction, although the energy distribution will depend on the absolute value of the second ϕ . Therefore MS is approximately the same at 5° and 136° . Similar conclusions have been reached in other studies of multiple scattering in slab geometry.²⁶ However, at low angles, there is very little single-scattering inelastic phonon intensity, so the nuclear inelastic scattering is completely dominated by the MS contribution. The satisfactory agreement between the LaCu_2Si_2 data and the Monte Carlo simulation at 5° (Fig. 2) confirms that the simulation is giving a reliable estimate of the MS intensity and this success has allowed us to assess the reliability of other procedures for determining the phonon contribution.

HO directly subtracted LaCu_2Si_2 data from CeCu_2Si_2 at 10 and 100 K after correction for the different scattering lengths. Their spectra suffer from poor statistics so that the phonon scattering is not very well defined. In addition, the low-temperature LaCu_2Si_2 spectra are estimated from measurements at 100 K. Attempts to perform a similar subtraction on the HET data immediately highlighted the main problem with this procedure; that the phonon peaks are shifted in energy in the two compounds. It is also clear that a uniform scaling of the entire spectrum by the total scattering power of the two samples may be a poor approximation. The main intensity difference is below 20 meV, whereas the scattering above 30 meV is nearly the same.

For this reason, HM applied a different technique which used the high-angle CeCu_2Si_2 data to define the

phonon contribution at low angle. They assumed that there would be no change in the energy distribution with angle, though since their high-angle data are at only 66° , with a still appreciable magnetic component, it is not clear how they defined unambiguously the shape of the PDOS. This method has the drawback that it neglects the effect of the higher-order scattering MS processes in distorting the spectral distribution especially at higher energy transfers, and may be the reason why they attributed extra intensity just below 40 meV to magnetic scattering. In our own analysis, this is seen to arise from peaks in the phonon scattering.

In our view, the safest method of estimating the phonon contribution is the procedure first described by Murrani.¹⁷ The LaCu_2Si_2 spectra are used to define a scaling function $R(\phi, \phi', \epsilon)$, which is the ratio at each ϵ of the measured intensities at low angle ϕ and high angle ϕ' (see Fig. 5). The phonon scattering in CeCu_2Si_2 at scattering angle ϕ is then given by multiplying the data at ϕ' by the same function $R(\phi, \phi', \epsilon)$. In this way, the shifts in the positions of the phonon peaks from the La to the Ce compound are not a problem, and the La data also permit an estimate of the spectral weight shift caused by MS. The only serious approximation involved is that the degree of MS is the same in both compounds. Provided that the samples have identical masses and geometry, this is reasonable since the difference in the total scattering strengths is only 14%. The Monte Carlo simulations have allowed us to determine the validity of this approximation and to conclude that any error is less than 4%, which is within the statistical uncertainties of the present experiment.

In the present experiment, we have used the ratio of the 5° and 136° measured intensities in LaCu_2Si_2 as the scaling function $R(5^\circ, 136^\circ, \epsilon)$, smoothed by a spline function in order to minimize statistical fluctuations. The CeCu_2Si_2 136° data were fitted phenomenologically to a series of Gaussian and Lorentzian line shapes which followed the measurements accurately, and the result was

multiplied by $R(5^\circ, 136^\circ, \epsilon)$. This estimate of the phonon contribution at $\phi = 5^\circ$ is the short-dashed line shown in Fig. 6, which shows that nearly all the intensity in the range 10 to 20 meV is due to phonon scattering.

As a further check on these conclusions, we have analyzed the KDSOG data in a similar way to HO. The LaCu_2Si_2 data were reduced by a factor of 0.91 which is the ratio of σ_i/M_i (see Ref. 27), and then subtracted from the CeCu_2Si_2 data, with the result shown in Fig. 4. As can be readily seen, this procedure does not work very well in the energy range 10 to 20 meV for the reasons already discussed. Phonon structure is still visible in the difference spectra because of the slight shifts in the phonon energies and the coarseness of the cross-section correction. The temperature dependence of this residual signal also confirms its phononic origin. The subtractions used by HO would have been subject to the same problem but could not be so readily identified because of the poor resolution. We have excluded the range 10 to 20 meV in our subsequent analysis of the magnetic scattering. In principle, a similar problem should affect the higher-energy silicon modes. However, the resolution on KDSOG in this energy range is not so good and the modes are much weaker. It has therefore not been necessary to eliminate this energy region as well.

B. Analysis of magnetic scattering

Having determined the magnetic contribution, we have fitted our data by using Eq. (2), convolved with the instrumental resolution functions appropriate to HET and KDSOG respectively. In both cases, we have represented the Van Vleck contribution as a single Lorentzian line shape, since inspection of the subtracted spectra does not justify further inelastic peaks (Fig. 6). HO propose that there is a second transition at 12 meV with half the intensity of the 30 meV peak. However, we estimate that the upper limit for any peak in this energy range is only 15%

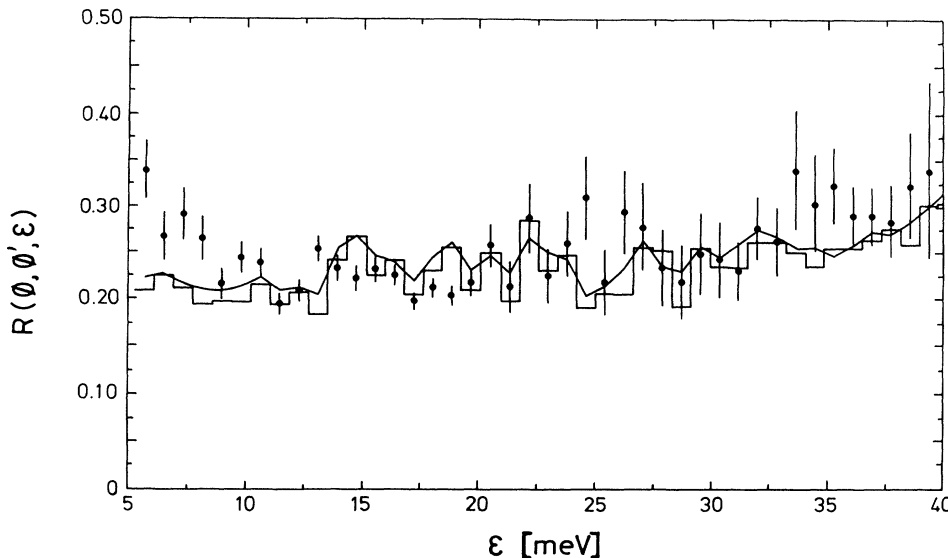


FIG. 5. A comparison of the scaling functions $R(\phi, \phi', \epsilon)$, $\phi = 5^\circ, \phi' = 136^\circ$, determined by Monte Carlo simulation for CeCu_2Si_2 (line) and LaCu_2Si_2 (histogram), and by experiment on LaCu_2Si_2 (points).

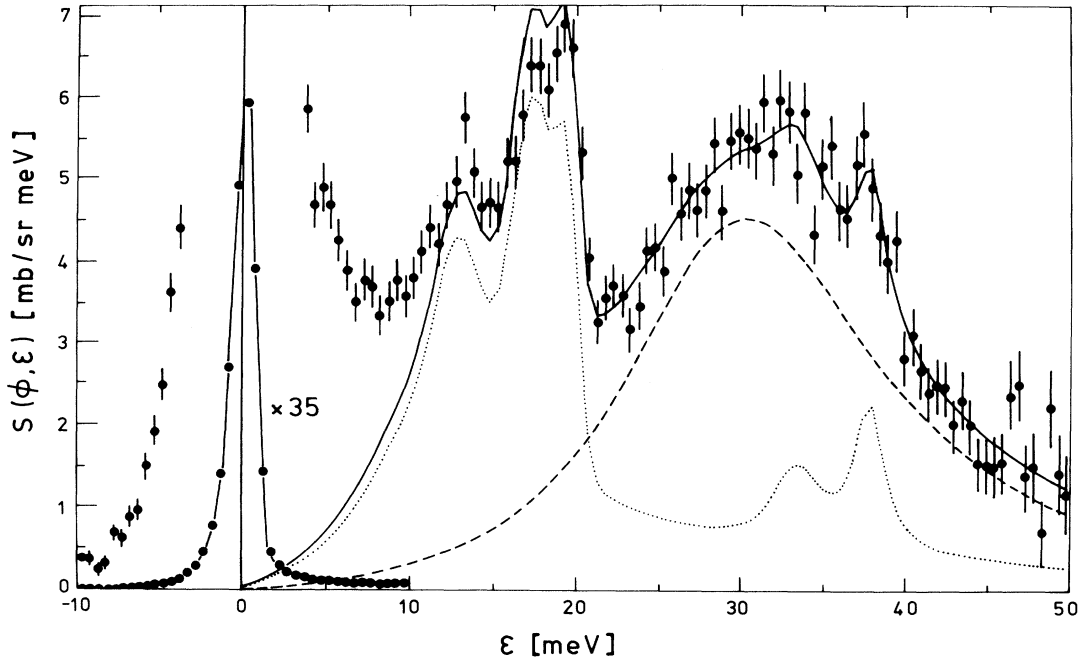


FIG. 6. Neutron energy spectra from CeCu_2Si_2 at 20 K measured on HET at 5° with an incident energy of 60 meV. The solid line is the sum of the phonon contribution estimated by the scaling function (short-dashed line) and the inelastic crystal-field excitation (long-dashed line).

of the 30 meV peak, assuming that it is not any broader. The fit of the HET data shows that the Lorentzian line shape gives a very good representation of the broadening of the CF transition. The solid line of Fig. 6 is the sum of this Lorentzian (long-dashed line) with the estimated phonon scattering (short-dashed line). This model correctly describes all features of the spectra including the small phonon peaks at 33 and 37 meV; there is only a small discrepancy in the region of the most intense phonon peak and we have not attempted to fit the QES. With the KDSOG data however, we have also been able to fit the magnetic QES component.

The fitted parameters of this scattering law are given in Table I where it can be seen that the HET and KDSOG data are consistent. The position of the CF transition is nearly temperature independent though the more accurate HET data suggest that there may be a small shift to

lower energy accompanied by a small increase in the linewidth on raising the temperature from 2 to 20 K. This is consistent with the Becker-Fulde-Keller model²⁸ but it may be an artifact of the subtraction procedure. The widths of the QES are in good agreement with previous measurements.^{8,10}

With the experimental configuration on HET, the CF transition was measured at wave-vector transfers between 1.6 and 2.7 \AA^{-1} . Over this Q range, there was no variation in the CF transition intensity, apart from a monotonic reduction due to the cerium form factor, or its linewidth. This observation, along with the Lorentzian line shape of the transition, suggests that dynamical relaxation is mainly responsible for the broadening of the CF peak rather than dispersion, although detailed single-crystal INS studies would be required to clarify this point.

TABLE I. Results of fitting Curie and Van Vleck susceptibilities to magnetic neutron scattering observed on HET and KDSOG. The susceptibilities of HET and KDSOG are normalized by the Van Vleck part at 20 K. χ_{MF} is the theoretical susceptibility of the proposed crystal-field model in the molecular-field approximation, using $\lambda = 52 \text{ mol/emu}$ (N.B. $1 \text{ emu/mol} = 0.0323 \mu_B^2/\text{meV}$).

T (K)		Curie part ($\varepsilon=0$)			Van Vleck part ($\varepsilon=\Delta$)		Total	
		χ (μ_B^2/meV)	Γ (meV)	Δ (meV)	χ (μ_B^2/meV)	Γ (meV)	χ (μ_B^2/meV)	χ_{MF} (μ_B^2/meV)
2	HET			30.0(0.3)	0.079(0.002)	8.4(0.4)		0.543
10	KDSOG	0.378(0.024)	1.9(0.1)	31.0(1.0)	0.079(0.008)	10.4(0.8)	0.457(0.025)	0.409
20	HET			29.4(0.2)	0.079(0.002)	9.3(0.4)		0.320
77	KDSOG	0.110(0.008)	4.4(0.3)	30.0(1.0)	0.087(0.008)	11.7(0.9)	0.197(0.011)	0.168
300	KDSOG	0.055(0.008)	7.4(0.7)	28.7(1.5)	0.039(0.008)	11.0(1.0)	0.095(0.011)	0.070

V. CF MODEL

Although a standard CF model is bound to be an oversimplification given the strength of the interactions between the cerium f states and the conduction band, it is interesting to see to what extent it can describe the experimental data. Since we have only measured one CF transition, it is not possible to determine the three parameters of the CF Hamiltonian from the neutron-scattering data alone [Eq. (1)]. However, the observation that the CF level scheme consists of a doublet and quartet (two close-lying doublets) places some strong constraints on the CF parameter values as can be seen in the following equations:

$$\begin{aligned} B_2^0 &= \frac{\Delta}{14} \left[\eta^2 - \frac{5}{6} \right], \\ B_4^0 &= \frac{\Delta}{210} \left[\eta^2 - \frac{1}{4} \right], \\ |B_4^4| &= \Delta \eta / 12 \sqrt{\frac{1}{5}(1-\eta^2)}, \end{aligned} \quad (3)$$

where Δ is the doublet-quartet splitting and η is a coefficient of the doublet wave function, i.e.,

$$|g.s.\rangle = \eta |\pm \frac{5}{2}\rangle \pm \sqrt{(1-\eta^2)} |\pm \frac{3}{2}\rangle,$$

where the $+$ ($-$) applies if B_4^4 is negative (positive). We further assume, on the basis of the specific-heat data, that the doublet is the ground state, i.e., $\Delta > 0$, so with Δ fixed to the experimental value, the CF potential depends on a single parameter η . This may be determined by fitting the single-crystal magnetic susceptibility data of Batlogg *et al.*⁴ since the measured anisotropy is approximately proportional to B_2^0 (Ref. 29) in the Curie-Weiss region. As shown in Fig. 7, the fit to our CF model (solid lines) gives good agreement, with values for the two adjustable parameters η and the molecular-field constant λ of 0.467 and 52 mol/emu, respectively. The HO model (dashed lines) cannot reproduce the measured anisotropy because

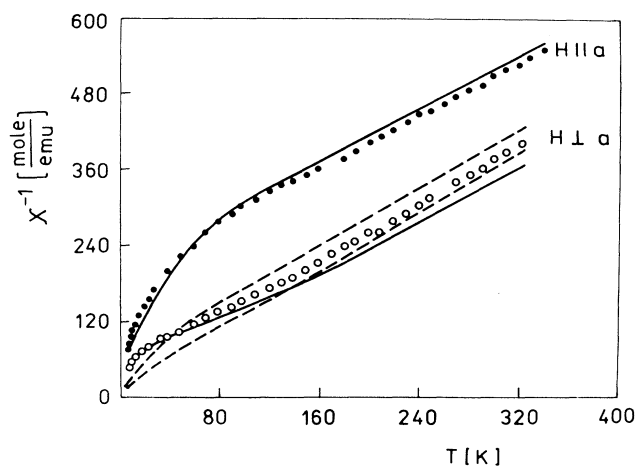


FIG. 7. Single-crystal bulk magnetic susceptibility of CeCu₂Si₂ [Batlogg *et al.* (Ref. 4)] compared to the current model using a molecular-field constant of 52 mol/emu (solid line) and to HO (dashed line).

its B_2^0 value is too small.

The CF parameters determined in this way with $\Delta = 29.4$ meV are

$$\begin{aligned} B_2^0 &= -1.29 \pm 0.06 \text{ meV}, \\ B_4^0 &= (-4.3 \pm 0.2) \times 10^{-3} \text{ meV}, \\ |B_4^4| &= 0.45 \pm 0.02 \text{ meV}. \end{aligned}$$

The temperature dependence of the CF transition intensity agrees well with the proposed CF model as shown by the solid line in the inset of Fig. 4. The dashed line shows the intensity variation of the HO CF model. The agreement with the new level scheme is especially significant since this particular test is insensitive to the details of the phonon subtraction, being based on scattering in regions of weak phonon intensity. The intensity is proportional to the population of the ground state so the fact that there is no reduction in intensity up to 77 K shows that the first excited level is at an energy of at least 30 meV.

Since the HET data are normalized on an absolute scale, it is possible to compare the static susceptibilities derived from the neutron data with the new CF model. The CF transition produces a Van Vleck susceptibility of $(7.3 \pm 0.4) \times 10^{-2} \mu_B^2/\text{meV}$ (the uncertainty arising from the estimated errors in the parameters), which is in reasonable agreement with the measured value of $(7.9 \pm 0.2) \times 10^{-2} \mu_B^2/\text{meV}$ providing further confirmation of the peak's CF origin. Since the Curie contribution could not be determined reliably on HET, we have normalized the KDSOG results to the HET data by assuming that the Van Vleck susceptibility does not change between 10 and 20 K (Table I). In order to compare the total susceptibility of the CF model with the neutron-derived value, it is necessary to apply a molecular-field correction, i.e., $\chi_{MF}^{-1} = \chi_{CF}^{-1} + \lambda$, where we have used the value of λ obtained from the fit to the single-crystal susceptibility. Once again, the agreement is satisfactory from 10 to 300 K. In particular, this shows that the ratio of the Curie and Van Vleck contributions to the dynamic susceptibilities is given correctly by the CF model.

It is worth noting that the need to introduce a molecular-field correction does not necessarily imply the existence of intersite exchange interactions, as sometimes stated, but is an inevitable consequence of the broadening of the CF levels, whether by single-site fluctuations or by dispersion. For example, a Curie-Weiss law ($\chi^{-1} \propto T + \theta$) is typically observed in dilute Kondo alloys with $\theta \sim T_K$,^{30,31} i.e., in the absence of intersite exchange. Holland-Moritz has given a detailed discussion of this point in Ref. 32.

With these parameters, it is possible to derive some information concerning the origin of the CF using Newman's superposition model (SM).³³ This assumes the CF potential to be the superposition of two-body potentials representing the interaction between the rare-earth ions and the individual nearest-neighbor ligands. It is therefore represented by two SM parameters (in the case of cerium), A_2 and A_4 , which are related to the B_n^m by

$$B_n^m = \Theta_n \sum_i \bar{A}_n(R_i) K_{mn}(\theta_i, \phi_i), \quad (4)$$

where Θ_n is the Steven's factor and (R_i, θ_i, ϕ_i) are the coordinates of the i th nearest-neighbor ligand. The geometrical coordination factors K_{mn} are defined in Ref. 33. In this way, the intrinsic strength of the CF, represented by the SM parameters \bar{A}_2 and \bar{A}_4 , may be separated from geometrical effects when the local ligand coordination is known. The validity of the SM is discussed in detail by Newman and Ng³³, who show that nearly all contributions to the CF potential, including overlap and hybridization, obey the superposition principle. Although it was developed to analyze the CF potential of ionic compounds, the neglect of more distant ligand contributions is likely to be a better approximation in metallic systems in which the CF is more effectively screened. In particular, the 4th degree parameters are dominated by short-range interactions and so our subsequent analysis depends only on B_4^0 and B_4^4 .

In the case of CeCu_2Si_2 , the cerium ion is surrounded by two nearly equidistant shells of eight silicon ions at 3.133 Å and eight copper ions at 3.218 Å (Ref. 34) (see Fig. 8). The contributions of the two shells to each of the CF parameters are given in Table II. In particular, the ratio of B_4^4 to B_4^0 may be used to determine the relative importance of each shell in the CF potential. Since the sign of B_4^4 is not known, there are two possible solutions for \bar{A}_4^{Si} and \bar{A}_4^{Cu} , both of which indicate that the silicon makes the stronger contribution to the potential by a factor of either 2.7 or 6.5.

Table II shows that the predicted ratio of B_4^4 to B_4^0 is 40.4 and -2.3 for the silicon and copper ligand contribu-

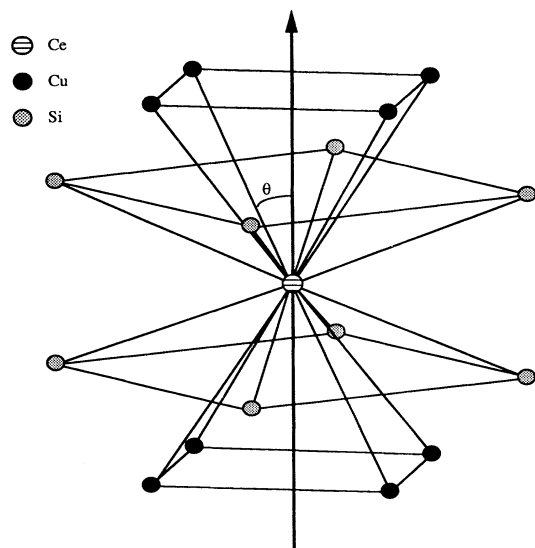


FIG. 8. Local coordination of cerium ions in CeCu_2Si_2 . θ is the polar angle of the ligand ion in the coordinate system used in the superposition model of the crystal-field potential [see Eq. (4)].

TABLE II. Superposition model analysis of crystal-field potential for CeCu_2Si_2 . B_n^m are the crystal-field coefficients of the Stevens' operators, α_J and β_J are the 2nd and 4th degree Stevens' factors, and \bar{A}_n^X are the intrinsic n th degree superposition model parameters for the ligand X . Values of \bar{A}_4^{Cu} and \bar{A}_4^{Si} are derived using $B_4^0 = -4.34 \times 10^{-3}$ meV and $|B_4^4| = 0.453$ meV.

$B_2^0 = \alpha_J$	$(3.143 \bar{A}_2^{\text{Cu}} - 2.249 \bar{A}_2^{\text{Si}})$	
$B_4^0 = \beta_J$	$(-2.456 \bar{A}_4^{\text{Cu}} - 0.632 \bar{A}_4^{\text{Si}})$	
$B_4^4 = \beta_J$	$(5.733 \bar{A}_4^{\text{Cu}} - 25.531 \bar{A}_4^{\text{Si}})$	
$B_4^4 > 0$	$\bar{A}_4^{\text{Cu}} = 0.943$ meV	$\bar{A}_4^{\text{Si}} = -2.58$ meV
$B_4^4 < 0$	$\bar{A}_4^{\text{Cu}} = -0.417$ meV	$\bar{A}_4^{\text{Si}} = 2.69$ meV

tions, respectively. The large ratio, in the case of the silicon contribution, arises because the SM coordination factor for B_4^0 (Table II in Ref. 33) is close to zero. The silicon polar angle θ in CeCu_2Si_2 is 67.6° , which may be compared with the value of 70.1° for which the coordination factor K_{40} is exactly equal to zero. B_4^4 , on the other hand, is proportional to $\sin^4\theta$ and so is much less sensitive to small changes in the ligand coordination angles. It is interesting to note that, in all the other isostructural $\text{Ce}T_2X_2$ compounds (T = transition metal, X = Si or Ge) for which CF parameters have been determined,^{35,36} B_4^0 is very small (in the case of CePd_2Si_2 , $B_4^0 = 0$ to within the experimental errors³⁶), whereas the B_4^4 are all in the range 0.24 to 0.45 meV and more accurately reflect the intrinsic strength of the CF. In particular, CeCu_2Ge_2 (Ref. 35) has an identical level scheme to CeCu_2Si_2 but with the energy scale reduced by a factor of 1.8. The close correspondence of the CF potential in all these compounds indicates that the X nearest-neighbor shell has the stronger influence.

VI. DISCUSSION

The previous analysis has produced a CF level scheme, with a doublet ground state and a quasiquartet at 30 meV, which is in agreement with all known CF-dependent experimental results (specific heat, single-crystal magnetic susceptibility, neutron scattering). The ratio of the Curie to Van Vleck terms in the dynamic magnetic susceptibility, as well as the derived static susceptibility, is also consistent with the CF model (Table I). It is perhaps surprising that a simple CF model works so well in this heavy-fermion compound in which the electronic properties are in other respects so remarkable. However, it appears that heavy-fermion systems only exhibit such anomalous behavior at low temperatures, i.e., on a low-energy scale. When viewed on a larger energy scale, the properties are more characteristic of localized f -electron systems affected by a CF potential. Nevertheless, the observed CF transition is extremely broad presumably because of the strong interactions of the f electrons with the conduction band and this broadening is much greater than the typical low-energy scales of CeCu_2Si_2 [$\Gamma_{\text{CF}} = 100$ K compared to estimated Kondo

temperatures of 8 K (Ref. 31)]. The order-of-magnitude difference in the linewidths of the QES (Table I and Refs. 8 and 10) and the CF transition is probably related to the increase in the number of hybridization channels with the high degeneracy of the excited level, as proposed by Lopes and Coqblin²⁰ but may also reflect differences in the hybridization matrix elements for states with different symmetry. It would be useful to perform a detailed theoretical calculation of the dynamic susceptibility of CeCu₂Si₂ using the new CF model.

We have concluded, on the basis of a SM analysis of the CF parameters that the silicon ligands make the principal contribution to the CF potential. The sign of \bar{A}_4^{Si} and \bar{A}_4^{Cu} cannot be unambiguously determined because the sign of B_4^4 is unknown. The evidence of other rare-earth intermetallic compounds^{37,38} is that \bar{A}_4 is always greater than zero, i.e., the 4th degree potential from neighboring ions is always repulsive to $4f$ electrons, as would be expected if short-range electrostatic and overlap interactions with ligand electrons are dominant. We have recently performed INS from NdCu₂Si₂ (Ref. 39) in which the overall CF splitting is only 11.5 meV. Performing a similar SM analysis, we find that the relative importance of the silicon and copper contributions to the 4th degree terms in the CF potential is reversed with $\bar{A}_4^{\text{Cu}} = 1.4$ meV (1.5 meV) and $\bar{A}_4^{\text{Si}} = 0.5$ meV (0.2 meV) when B_4^4 is positive (negative). Note that both parameters are now positive. In moving from NdCu₂Si₂ to CeCu₂Si₂, we find a significant increase in the magnitude of \bar{A}_4^{Si} whereas there is a smaller reduction in \bar{A}_4^{Cu} , suggesting that it is the silicon contribution that makes the CeCu₂Si₂ CF splittings anomalously large. If we therefore assume that the copper potential is of the same origin as in normal rare-earth compounds, we must prefer the solution with $\bar{A}_4^{\text{Cu}} > 0$, i.e., $B_4^4 > 0$ (Table II). The values of \bar{A}_4^{Cu} in the two compounds are then quite similar (0.9 meV in CeCu₂Si₂ and 1.5 meV in NdCu₂Si₂). On the other hand, \bar{A}_4^{Si} changes from a small positive value in the neodymium compound to a large negative value in the cerium compound. Although it is unusual to find $\bar{A}_4 < 0$, it is perhaps a consequence of the strong hybridization interactions that produce Fermi liquid behavior in the f electrons at low temperatures. A negative value indicates that the hybridization of the cerium f electrons and, presumably, the silicon p electrons produce a CF po-

tential that attracts $4f$ electrons towards the silicon ions.

Further confirmation of the anomalous character of the CF potential is provided by a comparison of our estimate of the B_2^0 parameter with another independent measure of the electric-field gradient in RCu_2Si_2 compounds (R = rare earth). Mössbauer studies of GdCu₂Si₂ would give a value of $B_2^0 = 1.76$ meV (Ref. 40) for the cerium compound after correction for all the necessary factors (Stevens factor, radial integral, and Sternheimer shielding factor). Allowing for all the uncertainties of such a scaling procedure, it is nevertheless significant that it is different in sign from the parameter deduced in the present work. If the CF potential were dominated by Coulomb interactions in both compounds, at least the signs should be the same⁴¹ as in rare-earth trifluorides for instance, whereas the effects of conduction-electron exchange can give rise to different signs, as seen in RNi_5 compounds.⁴²

An experimental investigation of other isostructural RCu_2Si_2 compounds is currently underway so that the systematic development of the CF potential across the rare-earth series is known. This should confirm that the large contribution of the silicon ligands in CeCu₂Si₂ is indeed anomalous in this series. The evidence presented in this paper that the CF splitting is produced by f - p hybridization suggests that there may be a scaling between the CF potential and the energy scale (e.g., the Kondo temperature) that characterizes the low-temperature properties of heavy-fermion compounds. It is interesting to note, for example, that both the strength of the CF potential and the transition linewidth of CeCu₂Ge₂ (Ref. 35) are substantially reduced compared to CeCu₂Si₂. The existence of the CeT_2X_2 series of isostructural compounds, in which the cerium ion is surrounded by two nearly equidistant shells of neighbors with very different electronic properties, provides a unique opportunity to test theories of the origin of the CF in anomalous rare-earth intermetallic compounds.

ACKNOWLEDGMENTS

We are grateful to Z. A. Bowden (RAL) and I. L. Sashin (JINR) for experimental assistance. E.A.G. would also like to acknowledge the Rutherford Appleton Laboratory for its hospitality and finance.

*Present address: Materials Science Division, Argonne National Laboratory, Argonne, IL 60439-4845.

¹F. Steglich, J. Aarts, C. D. Bredl, W. Lieke, D. Meschede, W. Franz, and J. Schafer, Phys. Rev. Lett. **43**, 1892 (1979).

²G. R. Stewart, Rev. Mod. Phys. **56**, 755 (1984).

³N. Grewe and F. Steglich, in *Handbook on the Physics and Chemistry of Rare Earths*, edited by K. A. Gschneidner, Jr. and L. Eyring (North-Holland, Amsterdam, 1991), Vol. 14, Chap. 97, p. 343.

⁴B. Batlogg, J. P. Remeika, A. S. Cooper, and Z. Fisk, J. Appl. Phys. **55**, 2001 (1984).

⁵Y. Onuki, T. Hirai, T. Komatsubara, S. Takayanagi, A. Sumi-

yama, A. Furukawa, Y. Oda, and H. Nagano, J. Magn. Mater. **52**, 338 (1985).

⁶J. Sticht, N. d'Ambrumenil, and J. Kübler, Z. Phys. B **65**, 149 (1986).

⁷P. M. Levy and S. Zhang, Phys. Rev. Lett. **62**, 78 (1989).

⁸S. Horn, E. Holland-Moritz, M. Loewenhaupt, F. Steglich, H. Scheuer, A. Benoit, and J. Flouquet, Phys. Rev. B **23**, 3171 (1981).

⁹E. Holland-Moritz, W. Weber, A. Severing, E. Zirngiebl, H. Spille, W. Baus, S. Horn, A. P. Murani, and J. L. Ragazzoni, Phys. Rev. B **39**, 6409 (1989).

¹⁰C. Stassis, B. Battlog, J. P. Remeika, J. D. Axe, G. Shirane,

- and Y. J. Uemura, *Phys. Rev. B* **33**, 1680 (1986).
- ¹¹Y. J. Uemura, C. F. Majkrzak, G. Shirane, C. Stassis, G. Aeppli, B. Batlogg, and J. P. Remeika, *Phys. Rev. B* **33**, 6508 (1986).
- ¹²C. D. Bredl, W. Lieke, R. Schefzyk, M. Lang, U. Rauchschalbe, F. Steglich, S. Riegel, R. Felten, G. Weber, J. Klaasse, J. Aarts, and F. R. de Boer, *J. Magn. Magn. Mater.* **47&48**, 30 (1985).
- ¹³N. Kawakami, T. Usuki, and A. Okiji, *J. Phys. Soc. Jpn.* **58**, 1427 (1989).
- ¹⁴S. Maekawa, S. Kashiba, S. Takahashi, and M. Tachiki, in *Theory of Heavy Fermions and Valence Fluctuations*, edited by T. Kasuya and T. Saso (Springer-Verlag, Berlin, 1985), p. 90.
- ¹⁵S. L. Cooper, M. V. Klein, Z. Fisk, and J. L. Smith, *Phys. Rev. B* **34**, 6235 (1986).
- ¹⁶F. Gompf, E. Gering, B. Renker, H. Rietschel, U. Rauchschalbe, and F. Steglich, *J. Magn. Magn. Mater.* **63&64**, 344 (1987).
- ¹⁷A. P. Murani, *Phys. Rev. B* **28**, 2308 (1983).
- ¹⁸E. Holland-Moritz, D. Wohlleben, and M. Loewenhaupt, *Phys. Rev. B* **25**, 7482 (1982).
- ¹⁹G. Zwicknagl, V. Zevin, and P. Fulde, *Z. Phys. B* **79**, 365 (1990).
- ²⁰L. C. Lopes and B. Coqblin, *Phys. Rev. B* **38**, 6807 (1988).
- ²¹S. Maekawa, S. Takahashi, S. Kashiba, and M. Tachiki, *J. Appl. Phys.* **57**, 3169 (1985).
- ²²M. W. Johnson, in DISCUS, *A Computer Program for the Calculation of Multiple Scattering Effects in Inelastic Neutron Scattering Experiments*, UKAEA Harwell Report AERE-R7682, 1974.
- ²³S. W. Lovesey, in *Theory of Neutron Scattering from Condensed Matter* (Clarendon, Oxford, 1984), Vol. 1, pp. 162–163.
- ²⁴R. Osborn (unpublished).
- ²⁵This justifies the use of the incoherent approximation, since the multiple scattering is dominated by processes with high Q , for which the approximation is most reliable.
- ²⁶V. F. Sears, *Adv. Phys.* **24**, 1 (1975).
- ²⁷J. M. Lawrence and S. M. Shapiro, *Phys. Rev. B* **22**, 4379 (1980).
- ²⁸K. W. Becker, P. Fulde, and J. Keller, *Z. Phys. B* **28**, 9 (1977).
- ²⁹P. Boutron, *Phys. Rev. B* **7**, 3226 (1973).
- ³⁰A. M. Tsvetick and P. B. Wiegmann, *Adv. Phys.* **32**, 453 (1983).
- ³¹N. B. Brandt and V. V. Moshchalkov, *Adv. Phys.* **33**, 373 (1984).
- ³²E. Holland-Moritz, *J. Magn. Magn. Mater.* **47&48**, 127 (1985).
- ³³D. J. Newman and B. Ng, *Rep. Prog. Phys.* **52**, 699 (1989).
- ³⁴T. Jarlborg, H. F. Braun, and M. Peter, *Z. Phys. B* **52**, 295 (1983).
- ³⁵G. Knopp, A. Loidl, K. Knorr, L. Pawlak, M. Duczmal, R. Caspary, U. Gottwick, H. Spille, F. Steglich, and A. P. Murani, *Z. Phys. B* **77**, 95 (1989).
- ³⁶A. Severing, E. Holland-Moritz, B. D. Rainford, S. R. Culverhouse, and B. Frick, *Phys. Rev. B* **39**, 2557 (1989).
- ³⁷D. J. Newman, *J. Phys. F* **13**, 1511 (1983).
- ³⁸M. Divis, *Phys. Status Solidi B* **164**, 227 (1991).
- ³⁹E. A. Goremychkin, A. Yu. Muzychka, and R. Osborn, *Physica B* **179**, 184 (1992).
- ⁴⁰G. Czjzek, V. Oestreich, H. Schmidt, K. Latka, and K. Tomala, *J. Magn. Magn. Mater.* **79**, 42 (1989).
- ⁴¹M. Budzynski, E. A. Goremychkin, O. I. Kochetov, A. Latuszynski, P. Mikolajczak, E. Mühle, A. I. Muminov, and M. Subotowicz, *Phys. Status Solidi B* **123**, 355 (1984).
- ⁴²E. A. Goremychkin and E. Mühle, *Pis'ma Zh. Eksp. Teor. Fiz.* **39**, 469 (1984) [*JETP Lett.* **39**, 570 (1984)].